Available online at www.sciencedirect.com

ScienceDirect

Procedia Engineering 69 (2014) 1232 – 1241

Procedia Engineering

www.elsevier.com/locate/procedia

24th DAAAM International Symposium on Intelligent Manufacturing and Automation, 2013

Force-Torque Control Implementation for 2 DoF Manipulator

Victor Titov*, I.Shardyko, Sergey Isaenko

Departament of robotic system design Russian State Scientific Center for Robotics and Technical Cybernetics, Saint-Petersburg, Russia

Abstract

This paper describes an approach to force control of two degrees of freedom robot manipulator. Aspects of control implementation concerning a joint torque sensor are discussed and a technique to its correction and calibration is presented. Two-level control scheme is used for the purposes of easier implementation. Such an approach has proved to be convenient in organizing general control structure and intrinsic to the two-time-scale dynamics of the system. For the fast part of system dynamics (corresponding to controlling the value measured by the torque sensor) joint model is presented. Based on this model, two variants of torque control loop are developed and their terms of application are outlined. Two types of control strategies for the slow part of system dynamics include an impedance control and force/torque control with gravity compensation as well as trajectory tracking based on the impedance control.

Keywords: torque sensor; force control; robot manipulator; callibration; zero reading fluctuation

1. Introduction

In the last decade the world has witnessed major advance in the field of force/torque control both practical and theoretical. Though, the first publications and experimental results concerning force/torque control can be dated down to the early 80s (and even earlier), the number of publications approaches its maximum from 2005 to 2009 and declining after that (according to [1-2]). Such a peculiar distribution may be explained as the result of recent improvements in microelectronics and computers power that makes it possible to implement the theoretical achievements in hardware. As one of such implementations worth mentioning is the outcome of DLR Institute of Robotics und Mechatronics hard work with their light-weight robots that uses impedance control framework [3-4].

Force/torque control consists of two central sub problems:

* Corresponding author. Tel.: +7-812-552-0110 ; fax: +7-812-556-3692 .
E-mail address: victortitov2005@mail.ru

doi:10.1016/j.proeng.2014.03.114

- Data acquisition – forces/torques in the wrist or just torques in the joints
- Control – incorporating this data into the control loop to enhance the overall quality of control

The former includes sensor design, calibration, measurement and preliminary data processing (filtering, correction). The later assumes the formulation of the control law that would use the force/torque data (along with other feedback) to achieve the expected robot behavior.

In this paper both problems are tackled to handle the control of 2 degrees of freedom (DoF) robot manipulator as an example of such systems. The robot is equipped with embedded torque sensors in each joint. Due to complex mechanical interaction within each joint, acquisition of the torque data faces a problem of additive distortion components present in the raw reading of the joint torque. This form the first goal of the paper as a search for the correction of the torque measurement that leads to elimination or reduction of additive distortions and increase accuracy.

The another problem consists of choosing the torque control law form at the joint level that corresponds to the upper level control strategies. In the present work two types of well-known upper level control strategies are tested: impedance control and force/torque control with gravity compensation. The control laws for the joint level have to meet the requirement of sufficient accuracy and transient behavior while saving the easiness of implementation and low computational complexity as well as be suitable for the upper level control strategies peculiarities. Though in theory a single optimal solution may be preferable, in practice, due to many factors influencing the control engineering, a universal solution is difficult to find. That happens to be true for the system discussed in the paper. Thus the second goal is the formulation of the joint level torque controllers that meet the requirements.

In the light of the problems stated the paper is organized as follows. First the hardware used is briefly described and the problems with data acquisition are outlined. Then several techniques of zero biases elimination are discussed and the optimal choice is made for microcontroller implementation. In the forth section the model of the flexible joint is presented in order to give necessary explanations for the control schemes in the fifth section. In the fifth section both the impedance and force/torque with gravity compensation control strategies of the upper control level are also mentioned. Finally the conclusion and discussions sum up the results and ways for future improvements.

2. Hardware used

2.1. Manipulator

The robot used in this work is two DoF planar robot manipulator (see fig. 1(a)). It consists of two mechatronic joint and a gripper (substituted for additional payload in the figure). Joints are made primarily of aluminium and linked with aluminium tubes in order to lower its weight. The total weight of the manipulator is 14 kg.

Due to universal electrical connectors and mechanical conjunctions the manipulator becomes reconfigurable. Each joint can be rotated about the previous links longitudinal axis with 45° step.

2.2. Joint

The joints are complete mechatronical modules. A torque drive accompanied with a strain wave gearing (with 100 and 160 reduction ratio for “elbow” and “shoulder” respectively) are embedded into an aluminum hull. Torque and position sensors are placed at the output shaft of the strain wave gearing. The position sensor has 0.006°/unit resolution (16 bit per rotation). The velocity feedback is acquired from the position feedback via numerical differentiation. The motor control is implemented on the Motorola’s MC56F8323 series hybrid 16-bit microcontroller (MCU). The external interface to the joint organized through 125 Kbit CAN interface.

2.3. Torque sensor

The torque sensor is a flange with three radial beams connecting the inner and outer rings as shown in the fig. 1(b). Microdisplacements in the material of the beams caused by the axial torque are measured with three pairs of stress gauges forming a half-bridge. The strain gauges are placed in such a way to minimize the influence of non-

axial torques and forces that are not aligned with the central axis of the sensor. The nominal torque of the both sensors (maximum design torque of the sensor) is 75 N•m.

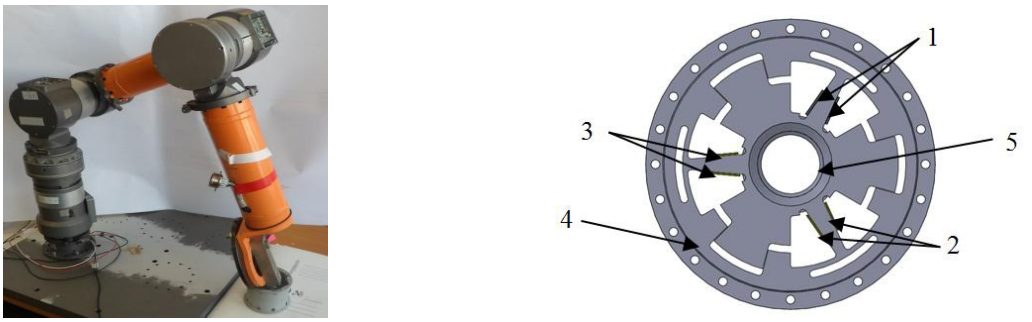

(a) (b)

Fig. 1. (a) – two degree of freedom robot manipulator with torque sensors in the joints; (b) – uni-axial torque sensor: 1-3 – strain gauge pairs forming half-bridges, 4 – outer ring, 5 – inner ring.

The same MCU as for the motor control with 12 bit ADC is used to measure three signals from operational amplifiers and output them to the motors microcontroller via I2C interface with 3kHz frequency (after preliminary filtration).

Being integrated within the joint and having no hull of its own the torque sensor is vulnerable to distortions caused by different parts of the joint mechanics interacting with the strain waver gearing output shaft where the torque sensor is placed. Due to these distortions the reading of the unloaded sensor fluctuates (zero reading fluctuation) as angular position of the joint changes. The zero reading fluctuation is shown in the fig. 2(a) against the angle of rotation. Fig. 2(b) shows the scaled region of the curve pointed in the fig. 2(a). It is clear from these two graphics that there is at least two types of distortions (apart from usual fixed bias) and presumably two major source of them.

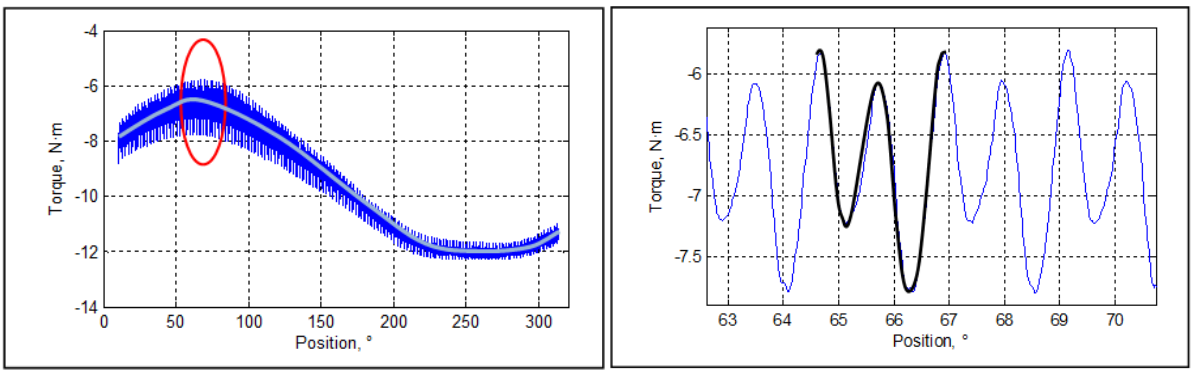

(a) (b)

Fig. 2. (a) – fluctuation of the unloaded torque sensor readings (*slow component*); (b) – scaled region of the Fluctuation of the unloaded torque sensor readings (*fast component* is shown in bold).

The first (slow) component (which is shown in the fig. 2(a) as an average fitting curve) changes slowly with the joint angular position and has the form close to sinusoidal. Apparently the source of this distortion component situates somewhere on the output shaft. The sensory data from three half-bridges show that the magnitude of this distortion in each signal is approximately the same but has phase shift for about 60° between any pair of signal out

of three. The most probable explanation for this is the output shaft curvature that makes the beams to bend along the rotation axes when all the strain gauges are subjected to approximately the same deformation. Although the true source can hardly be named since there is no means to disassemble and measure the deformation during the shaft motion.

The second (fast) component (shown in the fig. 2(b)) has many periods within one joint revolution. For the joint with 100 reduction ratio of the strain wave gearing the period of this curve is approximately 3.6° of the output shaft. As the analysis of sensory data from the three half-bridges show, this component of distortion manifests itself in all the three bridges having different sign, approximately the same magnitude but unstable phase shift between the three readings. One can assume that the source of this distortion component lies somewhere in the mechanical chain before the strain wave gearing or in the strain wave gearing itself. Thus exactly determining the source of this distortion component seems even less possible than that of the slow component.

Though the sources of the distortions are of great interest more important is a practical way to compensate them. In the next section several ways to correct the zero reading fluctuation are presented.

3. Torque Sensor Callibration And Zero Reading Fluctuation Compensation

From the description of the torque sensor given in the previous section two tasks arise.

The first is the correction of the sensor zero fluctuation. Being designed for the nominal torque of 75 N•m the sensor has the magnitude of the zero fluctuation for about 2.5 N•m (that is 3.3% of nominal range). This accuracy gives only 30 discreet steps of torque reading in one direction. Such a situation is not good enough for control purposes as well as for external torque registration.

The other task is to find the sensitivity of the sensor that converts measurement units into N•m (in the figures above this conversion has already been done for convenience of representation), i.e. calibration procedure.

3.1. Zero reading fluctuation compensation

Out of all possible ways to compensate the zero reading fluctuation the most reliable is the one using only the three signals from the half-bridges without adding any other feedback or assumptions about the distortions source models. Another requirement one may impose on this method is the compensation function to be a linear combination of the three signals from the half-bridges. It is just logical since the true relationship between the source zero reading fluctuation and its contribution to the three signal from the half-bridges stays unknown. In this situation the authors suggest to use the following as the output reading of the sensor (1)

$$u = k_0 + k_1 \cdot u_1 + k_2 \cdot u_2 + k_3 \cdot u_3 \quad (1)$$

where u_1, u_2, u_3 – signals from the three half-bridges; k_1, k_2, k_3 – scalar coefficients; k_0 – fixed magnitude offset. Taking into account the properties of the distortions one can determine the optimal values for k_1, k_2, k_3 to be equal 1. That makes the correction into the simple average of the three signals. No numerical optimization of k_0, k_1, k_2, k_3 gives any significant improvement for the system studied.

Unfortunately, this approach provides no more than 1.9 times reduction of the slow component and 1.2 of the fast component, in magnitude but adds harmonics to the curve due to summation of the three. This happens due to presence of non-sinusoidal components in the distortion.

Further reduction of the zero reading fluctuations can be done by looking for the nonlinear correction function of three variables or by approximating the curve with any method available and subtracting it from the output signal. The authors prefer the later as it is more transparent and easily tuned .

Three approximation techniques are considered to be applied: polynomial, piecewise polynomial, piecewise linear. To choose among this it is important to note that the function to be approximated depends on the angular position of the joint output shaft. Also the torque reading itself is required. Thus the only place where this computation can be done is the joints MCU where the motor control is performed and both values are available. As

this controller has excessive computational resources to spent on control purposes the optimal choice is piecewise linear approximation.

Points for piecewise linear approximation are chosen at the local minima and maxima of the fast component as shown in the fig. 3(a). There are totally 540 pair of points (positions, torque reading) for the joint with 160 reduction ratio. The pairs are arranged in two arrays of 2 byte values for torque and position. Array indexation is done via simple hash function that determines getting of the current shaft position into i-th interval in the position array. If current position is not close enough to one of the interval boundaries than the value of torque correction is computed according to (2)

$$T(x) = T_i + [T_{i+1} - T_i] \cdot [x_{i+1} - x_i] / [x - x_i] \quad (2)$$

where x – current position; T(x) – the value of correction; x_i, x_{i+1} – the beginning and the end of i-th interval; T_i, T_{i+1} – the correction value at the beginning and the end of i-th interval. This correction incorporates both the slow and the fast components. After the correction is applied the unloaded torque sensor reading fluctuation does not exceed 0.35 N·m (that is about 0.5% of the nominal torque). Fig. 3(b) demonstrates the unloaded torque sensor reading after correction against joint angular position.

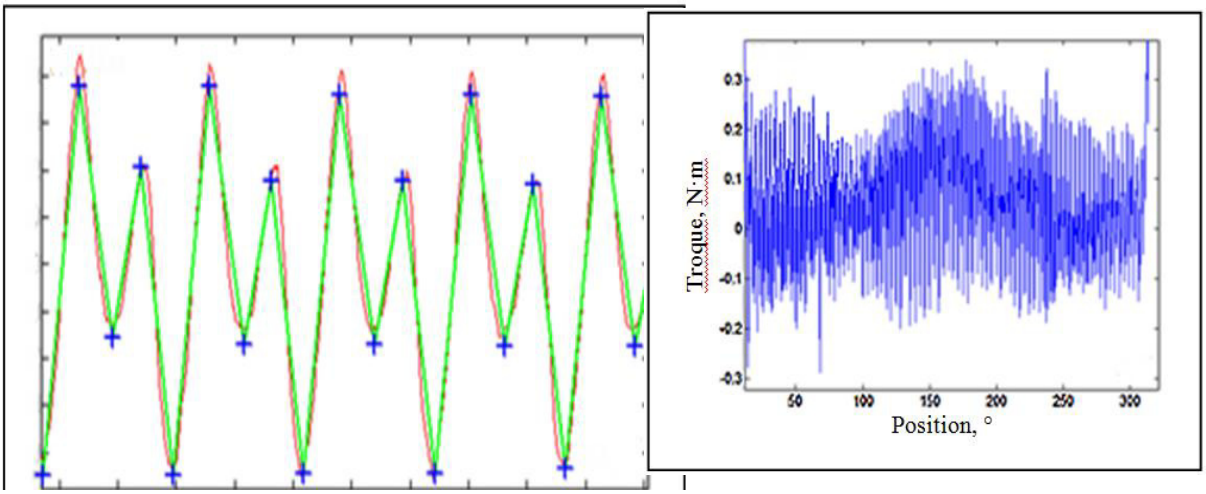

Fig. 3. (a) – scaled region of the zero reading fluctuation: points of approximation are marked as "+"; (b) – unloaded torque sensor reading fluctuation after correction.

3.2. Torque sensor calibration

The calibration procedure is performed by consequent loading of the torque sensor with increasing/decreasing payload. There have totally been performed ten series of increasing and decreasing loading cycles. First in one direction increasing series of loads was applied and the decreasing series was applied straight afterwards. Such cycles was repeated five times for each direction without alternating the direction for each series. The graphical representation of the results is show in the fig. 4. As one can see the sensor has good linear characteristic. The conversion coefficient used in all the figures above was calculated to be 145 unit/Nm. Some parameters of the torque sensor suggested in [5] a given in the Table 1.

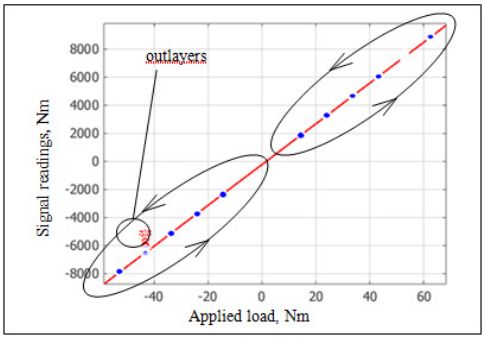

Fig. 4. Calibration graphic.

Table 1. Torque sensor parameters.

Parameters	Value
Sensitivity, units/N·m	145.58
Repeatability, units	119
Residual value at zero torque, units	18
Maximal deviation of indication from the fitting curve, units	259

4. Model of the joint with torque sensor

In this section a simplified mathematical model of the joint with torque sensor necessary is given for control schemes explanation purpose.

Although a torque drive is a synchronous 3-phase machine it can be approximated with the model of a standard DC motor (3).

$$\begin{cases} \tau_m(t) = C_m \cdot i_m(t); \\ e(t) = C_e \cdot \dot{\alpha}; \\ u(t) = e(t) + R_m \cdot i_m(t) + (di_m(t)/dt) \cdot L_m; \\ J_m \cdot \ddot{\alpha} = \tau_m(t) - \tau_{mext}(t) - \tau_{fric}(\dot{\alpha}, \tau_m - \tau_{mext}, t); \end{cases} \tag{3}$$

where τ_m – motor torque; C_m, C_e – electrical and torque constants of the motor; e – EMF; R_m , L_m – resistance and induction of the rotor; J_m – rotor inertia; τ_{mext} – external torque; $\ddot{\alpha}$, $\dot{\alpha}$ – second and first derivatives of the rotor angular position α , $\tau_{fric}(\dot{\alpha}, \tau_m - \tau_{mext}, t)$ – friction, u – supply voltage; i_m – motor current.

The friction force has two components: static and dynamic. The first represent the friction behavior before motion started. In general this can be expressed as (4) (see [6])

$$\tau_{fric} = \begin{cases} F(\dot{\alpha}, t), \text{ if } |\dot{\alpha}| > \Delta \\ \tau_m - \tau_{mext}, \text{ if } |\dot{\alpha}| \le \Delta, \ |\tau_m - \tau_{mext}| < F_S \\ F_S \cdot sign(\tau_m - \tau_{mext}), \text{otherwise} \end{cases} \tag{4}$$

where Δ – small value representing minimal velocity still deemed as zero; F_s – the value of static friction; $F(\dot{\alpha}, t)$ – dynamic friction model (in this work the LuGre model id used).

For simplicity the strain wave gearing is assumed to be infinitely stiff. The only compliant element in the system is the torque sensor. It is modeled as follows

$$\begin{cases} \tau = C \cdot (\alpha / r - q); \\ J_{load} \ddot{q} = \tau + D \cdot C^{-1} \cdot \dot{\tau} - \tau_{ext} \end{cases} \quad (5)$$

where C – the torque sensor stiffness ; J_{load} – payload inertia; D – viscous friction coefficient of the sensor material; τ – bending torque of the sensor; q – the angular position of the sensors output shaft; τ_{ext} – external torque applied to the sensor; r – reduction ratio.

Using (5) τ_{mext} in (3) is determines as (6)

$$\tau_{mext} = \tau + D \cdot C^{-1} \cdot \dot{\tau} \quad (6)$$

The graphical representation of the model is shown in the fig. 5.

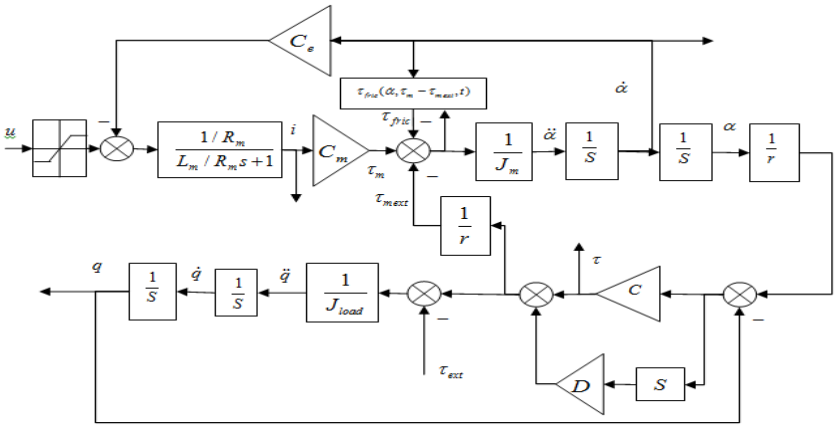

Fig. 5. Model of the joint with torque sensor (s = d/dt).

5. Approach to control

Force control is already a major field in robotics. The outline of the control strategies and their applications can be found in [7]. The control problems arising that can be met in literature mainly concern the elasticity of the torque sensor and its influence on the control dynamics. In a particular lots of authors point out two time scale dynamics of the flexible joint robot (FJR). The first model of elastic joint robot was proposed by Spong [8]. Since then numerous controllers was proposed some of which are outlined in [9].

In this work one of the classical robot control architecture including two (lower and upper) levels of control was adopted. The upper level of control generate required values of torque which are commanded to the lower level and processed by each joint independently. Such control architecture loses to the one with centralized computation in quality but wins significantly in simplicity while making module principle possible.

5.1. Joint level torque control

For the purposes of controlling the robot two types of torque controllers are used at the joint level. The torque control loop functioning at 1 kHz frequency while feedback is sampled and preprocessed at 3 kHz.

The first one is based on the research published in [10] and implements a passive adaptive torque controller. Assuming that the control of motor current is at least 10 times faster than the torque control loop (that is quite true) and one can command the required current directly neglecting the current transient, the torque controller can be expressed as (7)

$$i_d = K_{\tau i} \cdot \tau_d + K_{\tau i} \cdot K_p \cdot (\tau_d - \tau) - K_{\tau i} \cdot K_d \cdot \dot{\hat{\tau}} \tag{7}$$

where i_d – desired current value for the current control loop; $K_{\tau i}$ – conversion coefficient from current to motor torque; K_p – proportional gain; K_d – damping; τ – current value of the torque sensor measurements; τ_d – the desired torque produced by the upper level; $\dot{\hat{\tau}}$ – an estimation of the torque first derivative obtained using second order torque observer (8).

$$\begin{bmatrix} \hat{\tau}_{k+1} \\ \dot{\hat{\tau}}_{k+1} \end{bmatrix} = \begin{bmatrix} 1 & T_1 \\ 0 & 1 \end{bmatrix} \cdot \begin{bmatrix} \hat{\tau}_k \\ \dot{\hat{\tau}}_k \end{bmatrix} + \begin{bmatrix} l_1 & 0 \\ 0 & l_2 \end{bmatrix} \cdot (\tau - \hat{\tau}_k) \tag{8}$$

where l_1, l_2 – scalar coefficients ensuring required filtering level; T_1 – sampling period.

This controller has several qualities that make it convenient in application. First it is relatively simple and can be tuned intuitively by iteratively searching for its coefficients. It also has steady state (static) errorthat is both advantage and disadvantage of this controller. Although having static error makes this controller less preferable when accurate torque control is needed this error can be very useful when dealing with uncertainty of τ_d that frequently leads to the manipulator instability. An example of such instability is an attempt to compensate for gravity torque having uncertain mass parameters. Trying to feed the computed gravity torque to the torque controller in this case causes the manipulator to endlessly wander in search of the equilibrium point (where $\tau = \tau_d$). Thus the stability can't be ensured on the whole range of the joint positions. Having static error solves this problem at the cost of accuracy and system sensitivity.

The other controller uses inner velocity loop. It is fairly easy to see from the joint model in the fig. 5 that in the static case (when the output shaft of the sensor is blocked) controlling the torque reduces to controlling the position of the strain wave gearing output shaft. In general it is also true as the torque at the sensor can be expressed as the difference between the strain wave gearing output shaft position and the torque sensor output shaft position. Thus controlling the motor velocity is equal to controlling sensor torque derivative in the static case. In the control scheme proposed in this paper there is four control loops in linear hierarchy (the most inner loop is the first; see fig. 6):

- current loop;
- velocity loop that uses PI regulator to command the current loop;
- torque loop that uses P regulator to command the velocity loop;
- non linear damping loop that also commands the velocity loop.

Without additional damping the system gets the property of mechanical energy accumulator. Such system would hold its velocity until external torque is applied. To avoid this while saving good transient behavior the non-linear damping of the form (9) is applied.

$$\tau_{demp}(\dot{\alpha}, \tau, \tau_d) = \frac{K_D \dot{\alpha}}{k_{dec} |\tau_d - \tau| + 1} \tag{9}$$

where K_D – the maximal value of the damping coefficient; k_{dec} – coefficient determining how fast the damping is decreasing as the torque error is increasing. Such a damping offers good stability at the τ_d point while saving the sensitivity.

This controller has no static error and approximately the same stability as the first one. Such properties are the result of correction introduced by the inner loops (current, velocity). In the case of uncertain τ_d this controller is hardly applicable to gravity compensation since it would try to track τ_d no matter how far the true equilibrium is. When the fast and accurate torque control is needed this controller gives good results and is relatively easy to tune.

In the fig. 6 $\dot{\alpha}_d$ – the desired velocity for the velocity control loop; T1 – feedback sampling rate; T2 – velocity and torque control signal generation rate.

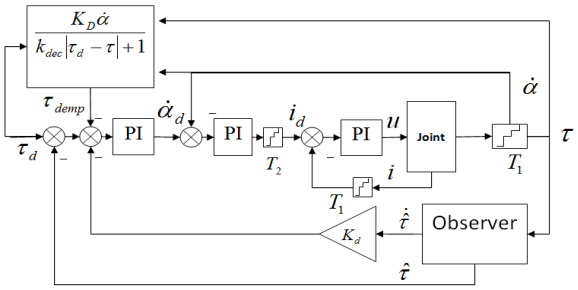

Fig. 6. Torque controller with inner velocity loop.

5.2. Upper level control

For this control level two types of control strategies are tested.

The first control strategy is the force/torque control with gravity compensation with additional damping. The desire torque vector (2 components) is formed as (10)

$$\tau_d = G(q) - K_{demp} \cdot \dot{q} \qquad (10)$$

where q – the vector of the sensors output shaft angular positions; $\dot{q}$ – the vector of its first derivatives; K_{demp} – damping factor; G – gravity torques computation function.

For this control strategy the passive adaptive torque controller is used due to the reasons discussed in the previous subsection. Main application of such a control strategy is to manually form a trajectory for the manipulator. The low accuracy of the joint level torque controller in this case poses certain difficulty for using the control strategy to command motion of exact force task (though if accuracy is not as important as safety this strategy can be used this way).

The other control strategy implemented on this level of control is partial impedance control. As known for example from [7] to fully implement impedance control one need to provide desired position along with its first and second derivatives as well as the same set of values in feedback. Acceleration measurement for the system has proved to be very difficult to obtain accurately. For this reason just limited version of impedance control is implemented (11).

$$\tau_d = G(q) + J(q)\cdot[S\cdot(q_d - q) + D\cdot(\dot{q}_d - \dot{q})] \qquad (11)$$

where J(q) – inertia matrix of manipulator (provides partial decoupling); S – proportional gain (or stiffness coefficient); D – damping factor; q_d – the vector of desired positions; $\dot{q}_d$ – the vector of its derivatives.

For this control strategy at the joint control level the controller of the second type (with inner velocity loop) is used. This strategy gives good positional accuracy (the better the bigger proportional gain S) and can provide significant compliance (without loss of accuracy if gravity compensation is computed). In dynamics (when $\dot{q} \neq 0$), providing control system with $\dot{q}_d$ significantly increases the accuracy of trajectory tracking at the cost of increasing complexity of the upper level. This control strategy is mainly used for safe manipulation tasks that requires considering the presence of unknown obstacles in the operational space.

In [11] another approach to the force-position control of the 8 DoF robotic arm is presented. In contrast with the system in the present paper only one 6 DoF force/torque sensor is placed at the wrist of the arm. The authors implemented a classical force control scheme with internal position-closed loop. Though good position and force tracking accuracy is granted the significant drawback of this approach is poor dynamic characteristics for force tracking (the approximate time constant is about 0.2 sec. while the time constant for our robot is less than 0.08 sec.). Poor dynamic characteristics in [11] are the result of closing the force loop on the upper control level which is much slower that used for position control. In our case the reverse scheme (with force/torque control at the lower level) proves to be more efficient.

6. Conclusion and discussions

In this paper, a complex of the problems concerning force/torque control was solve for a 2DoF robot manipulator used as example. Two major components of force/torque control for the robot was studied: torque data acquisition and control law formulation.

In the torque data acquisition a solution for the problem of zero reading fluctuation of a embedded toque sensor was presented. The proposed correction shows significant improvement of the sensors accuracy (the fluctuation magnitude decreased more than 7 times in comparison with the raw signal). For the torque sensor after zero reading correction the results of calibration procedure was presented.

Two joint level torque controllers were presented and discussed with their relation to the upper level control strategies. It was shown that static torque error introduces by a passive adaptive torque controller at the joint level ensures good stability properties when used with force/torque with gravity compensation control strategy at the upper level control. A torque controller with velocity inner loop shows no static error and better dynamic characteristics and proves to be useful in impedance control strategy.

Although the developed controllers from the basis for force/torque control they still lack certain properties that would give them wider application field. One of the serious problems in controlling manipulator with many degrees of freedom is significant dependence of the inertia parameters of the latter on the links positions. For the joint torque control system this leads to the changes in payload inertias with joints positions and as a result to the shift of the controllers optimal parameters. To handle this problem an adaptive mechanism should be applied in each joint to adjust the parameters. Adaptive structure of the joint torque controller can also enforce the module principle and make each joint interchangeable. Developing the adaptive controllers is one of the directions for the future work.

The correction of the torque measurement for the embedded sensor proposed in the papers generally improves the quality of the torque control but cannot be deemed as the final option since there is no guaranties that the form of compensation signal does not change with time. Ideally the elimination of the distortions sources would be the optimal solution. To achieve it the sensor construction should be reconsidered. Also, though in the present paper the zero readings fluctuation correction proved to be unremovable with just raw signals processing it doesn't mean that this rather attractive way cannot be used. Correct placement of the strain gauges (or/and probably adding several new strain gauges pairs) along with more complex signal processing may lead to much better results even without changing the sensor construction. The research of such possibilities is still to be done.

The development of the robot arm and the control system was carried out with the financial support of the Ministry of Education and Science of the Russian Federation.

References

[1] http://ieeexplore.ieee.org/search/searchresult.jsp?refinements%3D4291944822%2C4291944823%2C4291944245%2C4291944246%26ranges%3D1976_2014_p_Publication_Year%26rowsPerPage%3D100%26queryText%3Dforce+control+robotics&pageNumber=82

[2] http://www.mendeley.com

[3] A. Albu-Schäffer, S. Haddadin, Ch. Ott, A. Stemmer, T. Wimböck, G. Hirzinger, "The DLR lightweight robot: design and control concepts for robots in human environments", Industrial Robot: An International Journal, Vol. 34 Iss: 5, 2007, pp.376 – 385

[4] http://www.dlr.de/rm/en/desktopdefault.aspx/tabid-8017/

[5] EURAMET/cg-14/v.01: Guidelines on the Calibration of Static Torque Measuring Devices, rev.00, July, 2007

[6] Olsson H., Åström K.J., Canudas de Wit C., Gäfvert M., Lischinsky P., «Friction Models and Friction Compensation,» Eur. J. Control, т. Vol. 4, № 3, pp. 176-195, 1998.

[7] Siciliano, B., Sciavicco, L., Villani, L., Oriolo, G. Robotics. Modelling, Planning and Control, 2nd Printing., 2009, Springer-Verlag, XXIV, 632 p. 298 illus., ISBN 978-1-84628-641-4.

[8] Spong, M.W., "Modeling and Control of Elastic Joint Robots," J. Dyn. Syst., Meas., Contr.(1987).

[9] Ozgoli S., Taghirad H. D., "A survey on the control of flexible joint robots," Asian Journal of Control, Vol. 8, No. 4, pp. 1-15, December 2006.

[10] Albu-Schaffer A., Ott C., Hirzinger G., «A passivity based Cartesian impedance controller for flexible joint robots - part II: full state feedback, impedance design and experiments,» 2004.

[11] Giovanni Gerardo Muscolo, Kenji Hashimoto, Atsuo Takanishi, and Paolo Dario, "A Comparison between Two Force-Position Controllers with Gravity Compensation Simulated on a Humanoid Arm,"Journal of Robotics, vol. 2013, Article ID 256364, 14 pages, 2013. doi:10.1155/2013/256364.